Characterization of magnetron-sputtered partially ionized deposition as a function of metal and gas species

Monica M. C. Allain,[a] D. B. Hayden, D. R. Juliano, and D. N. Ruzic
University of Illinois, Urbana, Illinois 61801

(Received 5 October 1999; accepted 14 January 2000)

Conventional magnetron sputter deposition with a rf inductively coupled plasma (ICP) has demonstrated that ionized metal fluxes can be effectively utilized to fill trenches and vias with high aspect ratios. The ICP is created with a seven turn (1/2 wavelength), water cooled coil located between the magnetron cathode and the substrate. A large fraction of the metal atoms sputtered from the magnetron cathode are ionized by the ICP. These ions are accelerated across the sheath toward the substrate and deposited at normal incidence, by placing a negative bias on the substrate. A gridded energy analyzer configured with a quartz crystal microbalance is located in the center of the substrate plane to determine the ion and neutral deposition rates. While keeping the magnetron power, rf coil, target to substrate distance, pressure and diagnostic location constant, the ionization fraction was measured for two metal targets: Cu and Ti using three different working gases: Kr, Ar and Ne. Variations in target materials and working gases are shown to have an effect on ionization and deposition rates. The ionization rate is a sensitive function of the metal's ionization potential. The electron energy distribution in the plasma is affected by the sputtered metal and the working gases' ionization potential. © *2000 American Vacuum Society*. [S0734-2101(00)00603-5]

I. INTRODUCTION

Semiconductor metallization techniques such as physical and chemical vapor deposition have been utilized in the commercial production of integrated circuits. As circuit dimensions shrink and aspect ratios increase, these techniques are no longer desirable because of poor step coverage and void formation.[1] Conventional magnetron sputtering, a physical vapor deposition (PVD) process, utilizes metal atoms which are sputtered from a wide-area cathode. The angular distribution of the ejected atoms is roughly a cosine distribution that is further broadened by gas phase scattering. Since these sputtered atoms are primarily neutral their trajectory cannot be controlled by electric fields. Therefore to utilize magnetron sputtering for high aspect ratio features there are two possible solutions. One is based on the deposition of the neutral species which would involve directional filtering of the sputtered flux (i.e., collimated sputtering),[2] while the second is based on in-flight ionization of the sputtered or evaporated flux with subsequent acceleration of the metal ions to the sample by means of a substrate potential.[3]

The in-flight ionization of atoms is known as ionized physical vapor deposition (I-PVD). There are two inherent advantages to this technique over the conventional or collimated sputtering. First, all depositing ions arrive at normal incidence, which leads to directional deposition of the flux. Second, the depositing ions have an increased energy, which allows resputtering and reflection of the depositing flux leading to better sidewall conformality. In addition, this kinetic energy of the ions can be controlled at will simply by adjusting the relative potential difference between the plasma and the sample.

I-PVD has been demonstrated by introducing inductively coupled plasma (ICP) coil between the substrate and target and running at a higher pressure (25–70 mTorr) than collimated PVD.[4–6] In order to increase the electron temperature and density a rf power is applied to the coil. The ICP coil increases the ionization rate of the metal atoms which corresponds to an increase in the ionization fraction of the metal flux to the substrate. Previous experiments have used this method to characterize partially ionized aluminum deposition.[6] In that experiment a three turn coil was used to generate a rf plasma between the sputtering target and the substrate. Deposition rates and ionization fractions were obtained under several varying conditions. The conclusion of the experiment indicated that the added ICP coil provided plasma throughout a larger volume as well as raising the electron temperature and density, which lead to increased ionization of the sputtered metal flux. In this article we demonstrate I-PVD with a dc planar magnetron and report on the ionized deposition as a function of metal and gas species. Through the analysis of comparing materials and gas species we can learn more about the basic mechanisms involved in ionized deposition.

II. EXPERIMENT

A dc planar magnetron sputtering tool, with a 33-cm-diam rotating magnet and target, was used. A cross section of the chamber geometry, the ICP coil and the diagnostics are shown in Fig. 1. A seven turn, $\frac{1}{2}$ wavelength, water-cooled copper coil was powered by a 1.5 kW rf (13.56 MHz) power supply matched with a variable input capacitor (600–1200 pF) to maximize the coupling between the rf and dc plasma. The matching network consisted of three capacitors in parallel. One capacitor was fixed at 600 pF, the second capacitor was variable (0–600 pF) and the third capacitor was variable (0–150 pF). These capacitors were in series with the seven-

[a]Electronic mail: monica@starfire.ne.uiuc.edu

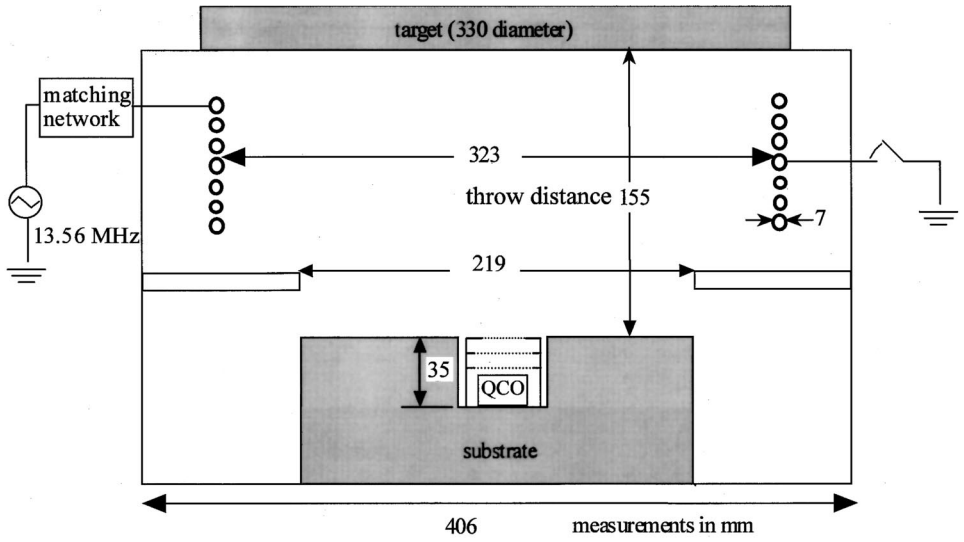

FIG. 1. Cross section schematic of the sputtering chamber. The casing which contains the quartz crystal oscillator (QCO) and the GEA is located within the substrate plane.

turn coil and were used extensively to minimize the reflected power from the coil. The coil was placed between the target and the substrate with a diameter of 31 cm ± 2 cm. To minimize the self-sputtering of the coil, the total length of the unwound coil was equal to $\frac{1}{2}$ wavelength of the rf. Then the center of the seven turn coil was grounded to allow one end of the coil to be powered while the other end floats. This allows the net dc voltage on the coil to be zero. The diagnostic used to measure the total and the neutral deposition rate of the metal flux consists of a quartz crystal microbalance (QCM) embedded under a three grid energy analyzer (GEA). The GEA consists of two adjustable biased grids and one nonadjustable. The nonadjustable top grid is placed over the opening of the casing and is biased with the substrate at −30 V. The middle and bottom grids are located inside the casing and are separated with a Teflon disk of 0.79±0.1 mm thickness. The inner and outer diameter of the Teflon disk is 23±1 and 32±1 mm, respectively. These grids are adjusted ±30 V to obtain the neutral and total deposition rates. When the two grids are biased at −30 V the total deposition rate (ions + neutrals) can be measured by the QCM, while the neutral deposition rate is determined when the bottom grid is biased +30 V. A LabVIEW program was utilized to produce a real-time plot of the deposition versus time using the QCM data. The slope of this plot is the total deposition rate when the grids are biased −30 V and it is the neutral deposition rate when the bottom grid is biased +30 V. The difference of these rates divided by the total deposition rate provides the ionization fraction. These diagnostics have been used in prior experiments and have been described in greater detail in previous articles.[7]

III. RESULTS AND DISCUSSION

The total source, the neutral and ion fractions, and the ionization fraction of the metal as a function of the working gas were determined by a diagnostic which consisted of a GEA and a QCM. The values were determined at the following constant parameters: magnetron power of 4 KW, rf power of 900 W, throw distance of 15.5 cm, gas pressure of 35 mTorr, and the diagnostic was located in the center of the substrate. Different targets and gases produce differing magnetic currents and voltages due to a number of factors. The current–voltage relationship in a magnetron appears to be strongly dependent on the ion induced secondary electron emission coefficient (γ) and partially dependent on the dynamics of the sputtered cathode atoms and the background gas. The γ is important for the following reason. As the voltage increases, γ rises leading to more electrons accelerated into the plasma. This causes more ionizations and therefore more sputtering and more electron emission.[8] The current–voltage relationship in a magnetron is also partially dependent on the rarefaction of the gas density near the cathode region. This occurs when the large fluxes of energetic sputtered atoms collide with the neutral gas and transfers energy. Since the pressure is constant the gas density decreases. The reduction in gas density results in a lower rate of ionizing collisions, thus the current on the cathode decreases and the voltage increases to maintain a constant magnetron power.[9,10]

To calculate the net metal influx, the VFTRIM3D code was used to determine the sputtering yields for the copper and titanium targets.[11] VFTRIM3D is based on the transport of ions in matter (TRIM) code, which utilizes a Monte Carlo model to simulate binary collisions within a solid. It tracks the cascade of atoms generated by an incident atom until they leave the surface or lose enough energy that they cannot escape. VFTRIM3D extends the TRIM concept to treat rough surfaces that are prescribed by a fractal model, with the fractal dimension varied to best match the roughness of the actual experimental surface. The sputtering yields obtained by VFTRIM3D at the experimentally determined voltages are shown in Fig. 2 with the symbol *Y* at each respective point. These experimentally determined yields are in agreement with published literature.[12]

The total source rate into the chamber, shown in Fig. 2, was obtained by taking the product of the sputtering yield

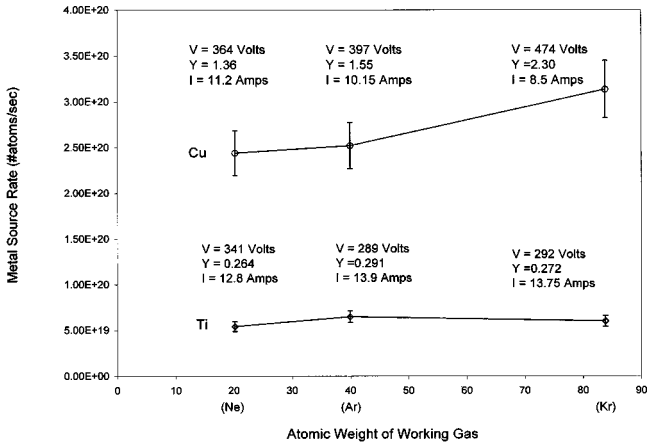

FIG. 2. Total source rate into the chamber vs metal source rate measured by the diagnostic (QCO and GEA) at 4 kW. Error bars are shown at every point.

and the ion current that strikes the target. The ion current that strikes the target and the voltage shown in this figure were measured by the magnetron power supply which was set at a constant power of 4 kW. Copper has a higher metal source rate than titanium because it has a higher sputtering yield. The yield is related to the momentum transfer from energetic particles to target surface atoms. The sputtered atoms must also overcome the surface binding energy of the targets. The bulk Debye temperature was used to obtain the surface binding energies of copper and titanium to be 3.52 and 4.89 eV, respectively.[13] The lower the surface binding energy, the lower the energy needed to sputter the material. Therefore copper, having the lower surface binding energy, has an even higher metal source rate into the chamber than titanium at the same magnetron power level.

Figure 3 shows the fraction of metal that reaches the bottom of a 1:1 via as neutral atoms. These data take into account the transmission of the three grids located in the GEA. Therefore the data represent the fraction of the metal that would reach the bottom of a 1:1 via as neutral atoms, in the absence of the three grids. The diagnostics, which were explained previously, determine the total number of atoms that

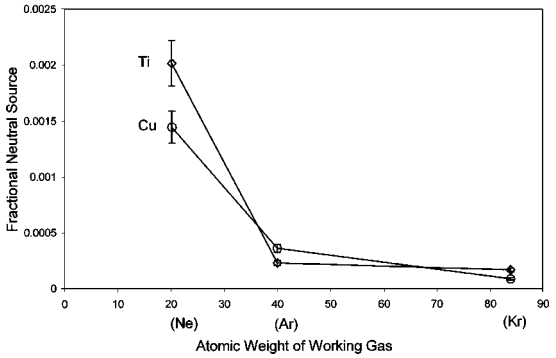

FIG. 3. Fraction of metal that reaches the bottom of a 1:1 via as neutral atoms provided by the GEA and QCM vs the fractional neutral source. Data have been normalized by the total amount of atoms sputtered into the plasma. Error bars are shown at every point.

TABLE I. Mean free paths of Cu and Ti in noble gases at 35 mTorr obtained from a slightly modified form of the momentum transfer cross section, where the differential cross section σ_e was calculated using a combination (see Ref. 14) of Lennard-Jones (see Ref. 15) and Ziegler–Biersack–Littmark Universal potentials (see Ref. 16).

Gas, 35 mTorr	Ti mfp (mm)	Cu mfp (mm)
Ne	4.4	6.9
Ar	2.0	2.6
Kr	1.2	1.6

reach the bottom of a 1:1 via; therefore we can also analyze what percent of the total number of atoms are neutrals by taking the neutral deposition and dividing it by the total. The data in Fig. 3 have been normalized by the total amount of atoms put into the plasma from Fig. 2. It shows that at most 0.2% of the metal put into the plasma make it down to the bottom of the via as atoms, while the remainder of the atoms are scattered to the sidewalls of the chamber or back to the target. A simple geometric diffusion model accounting for exponential attenuation based on a diffusion mean free path verifies the magnitude. This is why low pressures are typically used for deposition processes.

The effect of scattering is clearly evident in Fig. 3. As the mass of the working gas increases, the scattering increases, therefore the fraction of neutrals retaining a downward velocity, sufficient to reach the bottom of the via, decreases substantially. The metal experiences the least amount of scattering with neon compared to argon and krypton because it is the lightest working gas. The target to substrate distance is 15.5 cm while the mean free path of the gas atoms at a pressure of 35 mTorr is only a few millimeters, as shown in Table I.[14]

The mean free paths quoted are for momentum transfer, where the cross section used is a slightly modified form of the momentum transfer cross section commonly found in textbooks

$$\sigma_m = \frac{m_{\text{gas}}}{m_{\text{gas}} + m_{\text{metal}}} \int \sigma_e (1 - \cos\theta) \sin\theta \, d\theta,$$

where σ_e is the differential scattering cross section in the center of mass frame. Calculating σ_m in the center of mass frame with the prefactor containing the masses of the gas and metal atoms is necessary in order to integrate the actual momentum transferred in a collision. The standard definition of σ_m carried out in the lab frame without the prefactor is only correct in the limit of very light impacting particles on heavy targets (i.e., electrons on atoms). The differential cross section σ_e was calculated using a combination[14] of Lennard-Jones[15] and Ziegler–Biersack–Littmark ''Universal'' potentials.[16]

Figure 4 shows the fraction of metal that reaches the bottom of a 1:1 via as ions. These data were also obtained by the GEA and the QCM and the transmission of the grids were also taken into account. These data have been normalized to the total number of atoms put into the plasma. The fraction of ions that reach the bottom of the 1:1 via are a

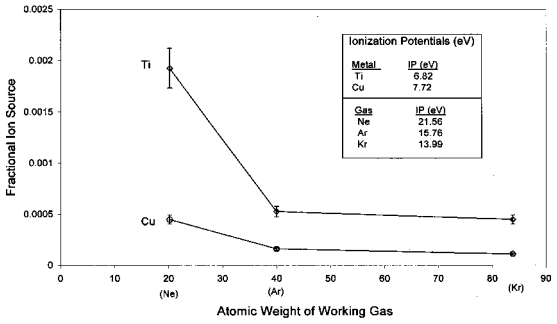

FIG. 4. Fraction of metal that reaches the bottom of a 1:1 via as ions provided by the GEA and QCM vs the fractional ion source. The data have been normalized by the total amount of atoms sputtered into the plasma. Error bars are shown at every point.

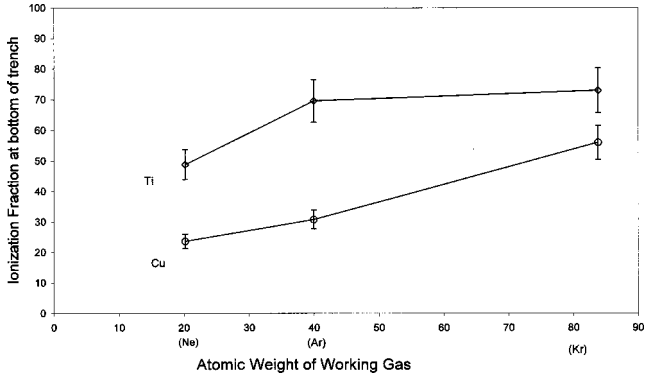

FIG. 5. Ionization fraction of metal at the bottom of a 1:1 via. Data have been normalized by the total amount of atoms put into the plasma. Error bars are shown at every point.

function of electron temperature and the ionization potential of the gas as well as the material of the target. The ionization potential is related to the amount of energy required to create one additional electron along with an ion from an inelastic collision between an electron and an atom. The working gas with the higher ionization potential requires more energy to be ionized and will therefore produce a higher electron temperature of the plasma. This effect was verified with an analytic model, which showed that the electron temperature for the neon working gas should be higher than that of argon and krypton.[14] This higher electron temperature will enable the energetic electrons to ionize more gas atoms thus increasing the sputtering of the target resulting in more metal entering the plasma. The higher electron temperature also ionizes more of the metal atoms thus leading to an increased ion fraction. This explains why the ion source decreases with decreasing working gas ionization potential (i.e., decrease in electron temperatures). There are more ionizations in Neon [ionization potential (IP=21.56 eV)] than Ar (IP=15.76 eV) and Kr (IP=13.99 eV). On the other hand, a lower metal ionization potential of the target material yields a higher fraction of ions in the plasma. Accordingly Fig. 4 shows that for a Ti target (IP=6.82 eV) with any working gas, the ion source is larger than the Cu target (IP=7.72 eV) with the same working gas. Although there are two effects of increasing ions in the plasma, the change in electron temperature for the various working gases will have the greatest impact on the number of metal atoms that are turned into ions.

A combination of the scattering and ionization effects is shown in Fig. 5. The ionization fraction is obtained by subtracting the total deposition rate (ions + neutrals) from the neutral deposition rate and dividing it by the total deposition rate. The Ti ionization fraction is higher than copper for all three working gases because the ionization potential for titanium is less than the ionization potential of copper. The graph has an increasing trend with increasing atomic weight of the working gas because of a combination of factors. As the mass of the working gas increases, fewer atoms reach the substrate because of increased scattering. The number of ions is also reduced, but not as greatly, due to the low ionization potential of the metal in combination with the high ionization potential (i.e., electron temperature) of the working gas. The net effect is a decrease in the denominator of the ionization fraction thus increasing the value of the ionization fraction.

IV. CONCLUSION

Characterization of ionized physical deposition as a function of metal and gas species has allowed an investigation into the basic mechanisms of this process. Although conventional magnetron sputter deposition with a rf inductively coupled plasma (ICP) has demonstrated that ionized metal fluxes can be effectively utilized to fill trenches and via with high aspect ratios,[17,18] understanding the basic physics is important in choosing the most effective ingredients for the perspective application at hand. The copper target with neon gas should be used in order to fill trenches with high aspect ratios because the ionization potential is higher for neon which yields a higher electron temperature, hence having the greatest impact on the number of metal atoms that are turned into ions in the plasma. The scattering is also significantly less due to the weight of neon versus argon and krypton.

ACKNOWLEDGMENTS

This research was funded by the NSF-DOE Basic Plasma Science Initiative. The dc-planar magnetron system was donated by Tokyo Electron, previously Materials Research Corporation. In addition, D. B. Hayden and D. R. Juliano were supported by Intel Fellowships. Special thanks and great appreciation specifically to Leslie Manohar for aiding with the data collection and figures.

[1]S. M. Rossnagel, Semicond. Int. 99 (1996).
[2]S. M. Rossnagel, D. Mikalsen, H. Kinoshita, and J. J. Cuomo, J. Vac. Sci. Technol. A **9**, 261 (1991).
[3]S. M. Rossnagel, J. Vac. Sci. Technol. B **16**, 2585 (1998).
[4]M. Yamashita, J. Vac. Sci. Technol. A **7**, 151 (1989).
[5]P. F. Cheng, S. M. Rossnagel, and D. N. Ruzic, J. Vac. Sci. Technol. B **13**, 203 (1995).
[6]D. B. Hayden, D. R. Juliano, K. M. Green, D. N. Ruzic, C. A. Weiss, K. A. Ashtiani, and T. J. Licata, J. Vac. Sci. Technol. A **16**, 624 (1998).
[7]K. M. Green, D. B. Hayden, D. R. Juliano, and D. N. Ruzic, Rev. Sci. Instrum. **68**, 4555 (1997).

[8]M. B. Hendricks, P. C. Smith, and D. N. Ruzic, J. Vac. Sci. Technol. A **12**, 1408 (1994).
[9]S. M. Rossnagel and H. R. Kaufman, J. Vac. Sci. Technol. A **6**, 223 (1988).
[10]S. M. Rossnagel, J. Vac. Sci. Technol. A **6**, 19 (1998).
[11]D. N. Ruzic, Nucl. Instrum. Methods Phys. Res. B **47**, 118 (1990).
[12]H. H. Andersen and H. L. Bay, in *Sputtering by Particle Bombardment 1*, edited by R. Behrisch (Springer, Berlin, 1981), p. 145.
[13]W. Eckstein, Computer Simulation of Ion-Solid Interactions (Springer, Berlin, 1991).
[14]D. R. Juliano, Ph.D. thesis, University of Illinois, 1999.
[15]S. Zhen and G. J. Davies, Phys. Status Solidi A **78**, 595 (1983).
[16]J. F. Ziegler, J. P. Biersack, and U. Littmark, *The Stopping and Range of Ions in Solids*, edited by J. F. Ziegler (Pergamon, New York, 1985), Vol. 1.
[17]S. M. Rossnagel and J. Hopwood, Appl. Phys. Lett. **63**, 3285 (1993).
[18]S. M. Rossnagel and J. Hopwood, J. Vac. Sci. Technol. B **12**, 449 (1994).